Article

Not peer-reviewed version

A Safer Alternative Bio-Repellent: Targeting Mosquito Odorant-Binding Proteins with Catnip-Derived Nepetalactones from *Nepeta cataria* Leaves

Tarawin Kiatlertpongsa , Jarupa Charoenrit , Jirawat Saetan , Supawadee Duangprom , Sineenart Songkoomkrong , Prateep Amonruttanapun , Piyapon Janpan , Prasert Sobhon , Sakda Daduang , Siriporn Nonkhwao * , Napamanee Kornthong *

Posted Date: 17 September 2025

doi: 10.20944/preprints202509.1531.v1

Keywords: *Nepeta cataria*; nepetalactones; odorant-binding proteins (OBPs); repellent; molecular docking; molecular dynamics simulation

Article

A Safer Alternative Bio-Repellent: Targeting Mosquito Odorant-Binding Proteins with Catnip-Derived Nepetalactones from *Nepeta cataria* Leaves

Tarawin Kiatlertpongsa [1], Jarupa Charoenrit [2], Jirawat Saetan [3], Supawadee Duangprom [2], Sineenart Songkoomkrong [2], Prateep Amonruttanapun [2], Piyapon Janpan [2], Prasert Sobhon [4], Sakda Daduang [5], Siriporn Nonkhwao [2,*] and Napamanee Kornthong [2,*]

[1] Ruamrudee International School, Minburi Campus, Bangkok 10510, Thailand
[2] Chulabhorn International College of Medicine, Thammasat University, Rangsit Campus, Pathumthani 12120, Thailand
[3] Division of Health and Applied Sciences, Faculty of Science, Prince of Songkla University, Hat Yai, Songkhla 90110, Thailand
[4] Department of Anatomy, Faculty of Science, Mahidol University, Bangkok 10400, Thailand
[5] Division of Pharmacognosy and Toxicology, Faculty of Pharmaceutical Sciences, Khon Kaen University, Khon Kaen 40002, Thailand
* Correspondence: siriphorn.nonkhaow@gmail.com; napamaneenatt@gmail.com

Abstract

The reliance on synthetic repellents such as N,N-diethyl-meta-toluamide (DEET) has raised health and environmental concerns, prompting the search for safer, plant-derived alternatives. Catnip (*Nepeta cataria* L.) is a rich source of iridoid monoterpenes, particularly nepetalactones, which are well known for their strong insect-repellent properties. However, the efficient extraction of nepetalactones remains challenging, and their precise mechanisms of action in insect inhibition are not yet fully understood. Thus, this study investigated the chemical composition from various methods, protein–ligand interactions, and pharmacokinetic safety profiles of catnip-derived compounds compared to DEET, with a focus on their interactions with odorant-binding proteins (OBPs) from *Anopheles gambiae* (*Agam*OBP), *Culex quinquefasciatus* (*Cqui*OBP), and *Aedes aegypti* (*Aaeg*OBP). Gas chromatography–tandem mass spectrometry (GC–MS/MS) confirmed the presence of nepetalactone isomers as the major constituents in catnip extracts obtained through stream distillation and dried leaves extracted in olive oil fractions. Molecular docking revealed that *cis,cis*- and *cis,trans*-nepetalactones and nepetalactone exhibited high binding affinities, surpassing those of DEET. Molecular dynamics simulations demonstrated that all OBP–ligand complexes achieved stable conformations. Notably, *cis,trans*-nepetalactone formed a more stable complex with *Agam*OBP than DEET. These findings suggest that nepetalactones stabilize OBP–ligand interactions while inducing subtle conformational flexibility, potentially disrupting mosquito odorant recognition in a manner distinct from DEET. ADMET predictions indicated that nepetalactones exhibit favorable absorption, distribution, and safety profiles with reduced predicted toxicity compared to DEET. Collectively, these results establish nepetalactones as promising candidates for the development of effective, safe, and sustainable plant-based repellents.

Keywords: *Nepeta cataria*; nepetalactones; odorant-binding proteins (OBPs); repellent; molecular docking; molecular dynamics simulation

1. Introduction

Vector-borne diseases remain a major global health challenge, with mosquitoes such as *Anopheles gambiae*, *Culex quinquefasciatus*, and *Aedes aegypti* serving as primary vectors for malaria, filariasis, dengue, Zika, and chikungunya [1,2]. The frontline strategy for reducing disease transmission has

 doi:10.20944/preprints202509.1531.v1

been the use of synthetic repellents, among which N,N-diethyl-meta-toluamide (DEET) remains the gold standard [3]. Although DEET has demonstrated broad-spectrum repellent efficacy across multiple insect species, its effectiveness, DEET has raised safety concerns, including neurological, cardiovascular, dermatological, and gastrointestinal adverse effects, particularly in children and individuals with repeated or prolonged dermal exposure [4–6]. Furthermore, the growing interest in eco-friendly and biodegradable alternatives underscores the urgent need for plant-derived repellents that combine efficacy with enhanced safety profiles [7,8]. One promising candidate is catnip (*Nepeta cataria* L.), a perennial herb of the Lamiaceae family. Traditionally valued for its medicinal properties and its euphoric effects in felines, catnip has recently attracted scientific attention for its strong insect-repellent activity [9]. Its essential oil contains iridoid monoterpenes, particularly nepetalactones stereoisomers such as *cis,trans*-nepetalactone, *cis,cis*-nepetalactone, and nepetalactone that account for up to 80% of the volatile fraction [10]. However, extracting nepetalactone and its derivatives is challenging and time-consuming. Notably, these compounds have demonstrated repellent activities against a range of arthropods, including mosquitoes, flies, ticks, and cockroaches, with some studies reporting efficacy equal to or exceeding that of DEET [11]. Nepetalactones activate the Transient receptor potential ankyrin 1 (TRPA1) receptor in *Aedes aegypti*, an ion channel associated with chemical nociception, thereby eliciting avoidance behavior [9].

Although the repellency of catnip and its nepetalactones has been demonstrated behaviorally, the molecular basis of their interaction with mosquito odorant-binding proteins (OBPs) remains insufficiently revealed. OBPs play a pivotal role in insect olfaction by binding and transporting semiochemicals to olfactory receptors, thereby mediating host-seeking behavior [12–14]. Structural and biochemical studies have shown that OBPs possess highly adaptable binding pockets capable of accommodating diverse ligands, and disruption of OBP–odorant interactions is a critical mechanism by which repellents interfere with host detection [15,16]. Comparative analyses of DEET and nepetalactones with OBPs of major disease vectors could therefore provide mechanistic insight into their mode of action and inform the rational design of next-generation bio-repellent. Specifically, this study aims to compare different extraction methods to identify the approach that provides the highest yield, employs a simple procedure, and utilizes green solvents. Next, to evaluate the comparative binding affinity and conformational effects of nepetalactone isomers and DEET on mosquito OBPs [17]. The findings highlight how nepetalactones may induce flexibility or stabilization within OBP binding pockets, providing a molecular basis for their repellent efficacy. In addition, the favorable pharmacokinetic and toxicological properties of nepetalactones support their potential as safer alternatives to DEET [18].

To address this knowledge gap, the present study employed a multifaceted approach, integrating gas chromatography–tandem mass spectrometry (GC–MS/MS) to profile phytochemicals obtained through different extraction methods, molecular docking, and molecular dynamics simulations to assess interactions with OBPs from *Anopheles gambiae* (*Agam*OBP, PDB ID: 3N7H), *Culex quinquefasciatus* (*Cqui*OBP, PDB ID: 3OGN), and *Aedes aegypti* (*Aaeg*OBP, PDB ID: 3K1E), and ADMET prediction to evaluate pharmacokinetic and toxicological properties. By combining computational, chemical, and toxicological perspectives, this study provides an in-depth evaluation of catnip-derived nepetalactones as potential bio-repellents. The findings not only expand our mechanistic understanding of insect repellency but also contribute to the development of safer, sustainable, and plant-based alternatives to synthetic repellents.

2. Results

2.1. GC–MS/MS Identification of Catnip Extracts

The compound composition of *Nepeta cataria* extracts obtained via three different extraction techniques, including stream distillation (SDE) and maceration methods, including fresh leaf in olive oil extraction (FOE) and dried leaf in olive oil extraction (DOE), was analyzed using GC–MS/MS (Figure S1) [19]. The findings demonstrated that the extraction approach exerted a pronounced

 doi:10.20944/preprints202509.1531.v1

influence on qualitative profiles of volatile and semi-volatile constituents, including hydrocarbons, oxygenated volatiles, esters, phenolics, terpenoids, and iridoid lactones (Table 1).

Across both leaf macerations in oil extraction types, the predominant compound was identified as butylated hydroxytoluene (BHT), with relative abundances 31.80% in FOE and 18.22% in DOE. In DOE, caryophyllene (0.12%) was identified as the only terpene in this fraction. Next, hydrocarbon constituents, particularly alkanes such as undecane, 2,6-dimethylnonane, and heptadecane, were also consistently abundant. FOE exhibited a higher alkane content (26.97%) compared to DOE (22.80%). Notably, the olive oil-based used in both FOE and DOE contained about 41.53% alkanes, contributing to their overall composition. Oxygenated aliphatic alcohols were detected in appreciable relative area, with 3,7-dimethyl-1-octanol reaching 4.11% and 2-isopropyl-5-methyl-1-heptanol reaching 3.48%, both enriched in FOE. Esters such as tetrahydrogeranyl formate were also relatively abundant FOE (4.48%). However, nepetalactones were completely absent, likely due to the high water content in fresh leaf conditions. FOE and DOE favored the recovery of oxygenated volatiles, esters, and phenolic antioxidants. Most notably, DOE and SDE yielded iridoid lactones, recognized as the hallmark bioactive constituents of catnip with established insect-repellent properties. GC–MS/MS can separate and tentatively identify *cis,cis*- and *cis,trans*-derivatives based on their differing retention times, as compared with reference standards and literature report [20,21]. SDE fraction included *cis,trans*-nepetalactone; *cis,trans*-NL (52.80%) and *cis,cis*-nepetalactone; *cis,cis*-NL (47.20%) as major compositions. DOE fraction found *cis,trans*-NL (4.90%), *cis,cis*-NL (1.80%), and NL (0.24%).

Interestingly, DOE produced the broadest spectrum of compounds, particularly nepetalactone isomers, highlighting it as a green and efficient method for isolating bio-repellent constituents from *N. cataria*. Notably, olive oil maceration also represents a simple, eco-friendly, and rapid extraction method, with potential synergistic contributions from hydrocarbons, oxygenated volatiles, and phenolic compounds [22]. Nevertheless, the highest yields of nepetalactones were obtained from steam distillation.

Table 1. Compound composition of *N. cataria* identified by GC–MS/MS from stream distillation (SDE) and from fresh (FOE), dried leaf oil extractions (DOE), and olive oil.

Compound	Formula	RT (min)	% Peak area			
			SDE	FOE	DOE	Olive oil
Polycyclic Alkane						
trans-4a-Methyl-decahydronaphthalene	$C_{11}H_{20}$	10.48	0	0.84	0.27	1.16
2-Methyldecahydronaphthalene	$C_{11}H_{20}$	11.18,11.08	0	1.27	0.69	1.31
1,6-Dimethyldecahydronaphthalene	$C_{12}H_{22}$	12.97	0	0	0.45	0
Cycloalkane						
trans-1,4-Dimethylcyclooctane	$C_{10}H_{20}$	9.04	0	0	0	6.86
Pentylcyclohexane	$C_{11}H_{22}$	11.5	0	1.45	0.39	1.29
1,4-Dimethyl-2-octadecylcyclohexane	$C_{26}H_{54}$	46.92	0	0	0.59	0
Alkene						
2,4-Dimethyl-1-heptene	C_9H_{18}	3.14	0	14.18	4.36	22.2
(2*Z*)-7-Methyl-2-decene	$C_{11}H_{22}$	7.04,6.97	0	0	0.33	1.35
(3*E*)-3-Heptadecene	$C_{17}H_{34}$	41.73	0	0	1.50	0
1-Tetracosene	$C_{24}H_{48}$	45.9	0	0	0.33	0
1-Hexacosene	$C_{26}H_{52}$	46.51	0	0	0.77	0
Alcohol						
3,7-Dimethyl-1-octanol	$C_{10}H_{22}O$	9.13	0	4.11	1.73	0
2-Butyloctanol	$C_{12}H_{26}O$	20.58,20.5	0	3.02	1.78	3.08

 doi:10.20944/preprints202509.1531.v1

2-Isopropyl-5-methyl-1-heptanol	$C_{11}H_{24}O$	21.08,20.95	0	3.49	2.51	4.05
11-Methyldodecanol	$C_{13}H_{26}O$	21.43	0	0	0	3.01
2-Methyl-1-decanol	$C_{11}H_{24}O$	21.55	0	2.56	1.90	0
3,7,11-Trimethyl-1-dodecanol	$C_{15}H_{32}O$	33.21	0	0	0.56	0
2-Hexyldecanol	$C_{16}H_{34}O$	33.77	0	0	0.60	0.91
2-Hexyl-1-octanol	$C_{14}H_{30}O$	34.78,33.1	0	1.49	0.94	0.87
2-Octyl-1-dodecanol	$C_{20}H_{42}O$	35.35	0	0	0.71	0
2-Hexyldodecanol	$C_{18}H_{38}O$	44.99	0	0	0.40	0
2-*cis*-9-Octadecenyloxyethanol	$C_{20}H_{40}O_2$	55.74	0	0	0.65	0
Ester						
Tetrahydrogeranyl formate	$C_{11}H_{20}O_2$	9.3,9.22	0	4.48	1.94	7.57
Carbonic acid, eicosyl vinyl ester	$C_{23}H_{44}O_3$	48.23	0	0	0.60	0
Glycidyl (Z)-9-Heptadecenoate	$C_{20}H_{36}O_3$	60.62	0	0	0.87	0
Glycidyl palmitate	$C_{19}H_{36}O_3$	62.54	0	0	10.77	0
9-Octadecenoic acid (Z)-, oxiranylmethyl ester	$C_{21}H_{38}O_3$	62.72	0	0	5.45	0
Sulfonamide						
N-(2-Hydroxyethyl)-N-methyl-perfluorobutane-1-sulfonamide	$C_7H_8F_9NO_3S$	15.85	0	1.87	0	0
Aromatic Hydrocarbon						
1,3-Di-tert-butylbenzene	$C_{14}H_{22}$	17.63	0	0	4.71	0
Lactone (Iridoid)						
cis-trans-Nepetalactone	$C_{10}H_{14}O_2$	23.58	52.80	0	4.90	0
cis,cis-Nepetalactone	$C_{10}H_{14}O_2$	25.21	47.20	0	1.80	0
Nepetalactone	$C_{10}H_{14}O_2$	25.58	0	0	0.24	0
Sesquiterpene						
Caryophyllene	$C_{15}H_{24}$	26.99	0	0	0.12	0
Aromatic Ketone						
4-Methoxy-3-(isopenten-2-yl)acetophenone	$C_{13}H_{16}O_2$	30.52	0	2.05	1.35	0
Butylated Hydroxytoluene	$C_{15}H_{24}O$	32.5,32.39	0	31.79	18.22	4.81
Unsaturated Fatty Acid						
6-Octadecenoic acid	$C_{18}H_{34}O_2$	58.47	0	0	0.61	0
Oleic Acid	$C_{18}H_{34}O_2$	59.97	0	0	0.75	0
9-Octadecenoic acid	$C_{18}H_{34}O_2$	61	0	0	0.49	0
(*E*)-13-Docosenoic acid	$C_{22}H_{42}O_2$	61.48	0	0	0.49	0
cis-13-Eicosenoic acid	$C_{20}H_{38}O_2$	61.66	0	0	1.03	0
cis-11-Eicosenoic acid	$C_{20}H_{38}O_2$	62.14	0	0	0.83	0
Alkane group						
		3.43-54.91	0	26.97	22.80	41.53

 doi:10.20944/preprints202509.1531.v1

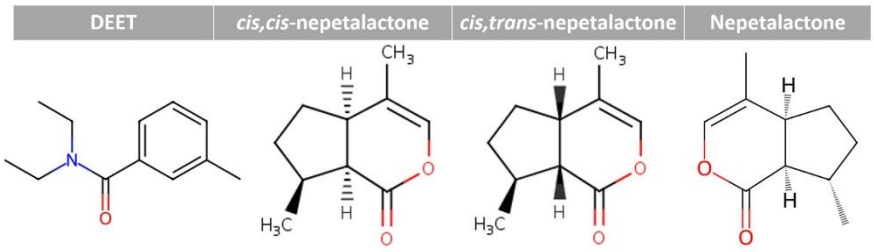

Figure 1. Chemical structures of DEET and nepetalactones.

2.2. Structural Analysis of OBP Receptors

The three-dimensional structures and mature amino acid sequences of *Anopheles gambiae* OBP (*Agam*OBP, PDB ID: 3N7H), *Culex quinquefasciatus* OBP (*Cqui*OBP, PDB ID: 3OGN), and *Aedes aegypti* OBP (*Aaeg*OBP, PDB ID: 3K1E) were obtained from the RCSB Protein Data Bank (RCSB PDB) to characterize their structural organization and suitability as receptor targets for bio-repellent docking [23]. All three proteins adopted the canonical OBP fold, consisting of six α-helices (α1–α6) that surround a central hydrophobic binding pocket (Figure 2A–C). This conserved helical scaffold is stabilized by three disulfide bridges, which are essential for maintaining the structural integrity of the ligand-binding cavity. Despite their overall structural similarity, subtle differences were observed in the orientation of helices α4–α6 and the dimensions of the binding pocket, which may contribute to variation in ligand recognition across mosquito species. *Agam*OBP displayed a relatively compact binding cavity, while *Cqui*OBP presented a slightly wider pocket, and *Aaeg*OBP exhibited an elongated hydrophobic groove, suggesting differential adaptability to diverse ligands. The sequence alignment of the three OBPs revealed high conservation across key residues, particularly the six cysteines that form disulfide bridges, as well as several hydrophobic residues that line the ligand-binding channel. Conserved motifs such as the Phe-Leu-Ala region and Lys-Cys-Tyr cluster were consistently present, underscoring their functional role in stabilizing protein folding and ligand interaction (Figure 2D). The overall sequence identity further confirms the evolutionary conservation of OBPs among mosquito species.

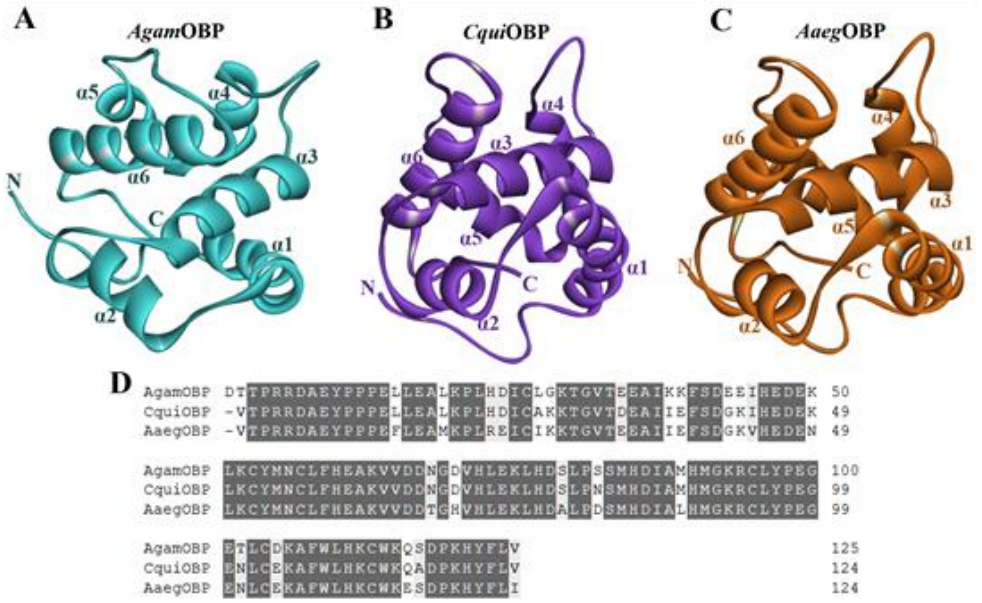

Figure 2. (A–C) Three-dimensional structures of *Agam*OBP, *Cqui*OBP, and *Aaeg*OBP, respectively. **(D)** Amino acid sequence alignment of the OPBs.

 doi:10.20944/preprints202509.1531.v1

2.3. Molecular Docking of DEET and Nepetalactone Isomers with OBPs

The binding affinities of DEET and nepetalactone derivatives with *Agam*OBP, *Cqui*OBP, and *Aaeg*OBP, were assessed using AutoDock Vina (Table 2) [25,26]. DEET, the reference synthetic repellent, exhibited moderate binding scores of −6.4, −6.3, and −6.2 kJ/mol with *Agam*OBP, *Cqui*OBP, and *Aaeg*OBP, respectively, indicating relatively uniform but modest affinity across the three receptors. In contrast, nepetalactones demonstrated stronger interactions with all OBPs. *Cis,cis*-NL bound more tightly than DEET, with docking scores of −6.6, −6.6, and −7.0 kJ/mol, the strongest interaction occurring with *Aaeg*OBP (−7.0 kJ/mol). Similarly, *cis,trans*-NL showed consistent affinity −6.6, −6.7, and −6.7 kJ/mol across *Agam*OBP, *Cqui*OBP, and *Aaeg*OBP, respectively, suggesting a stable binding profile irrespective of receptor type. NL form also exhibited higher binding than DEET, with scores of −6.7 (*Agam*OBP), −6.6 (*Cqui*OBP), and a maximum of −7.0 kJ/mol with *Aaeg*OBP. Collectively, these results indicate that all nepetalactones outperform DEET in binding affinity, with *Aaeg*OBP consistently displaying the strongest interactions. Analysis of binding pocket volumes revealed notable structural variability among the three OBPs. The cavity of *Agam*OBP was the smallest (1159 Å³), while *Cqui*OBP possessed the largest cavity (1643 Å³), and *Aaeg*OBP displayed an intermediate size (1284 Å³). These differences in cavity architecture may influence ligand accommodation and selectivity, with larger or more flexible pockets potentially allowing stronger stabilization of bulky or conformationally diverse ligands such as nepetalactones. Interestingly, molecular docking was performed with ligands identified across all fractions, including FOE, DOE, and olive oil, against the *Agam*OBP, *Cqui*OBP, and *Aaeg*OBP receptors. Several ligands, such as 2,6,10-trimethyldodecane, 2-methyldecahydronaphthalene, butylated hydroxytoluene, and *trans*-4a-methyl-decahydronaphthalene, exhibited equal or higher binding affinity to all receptors compared with DEET and nepetalactones (Table S1). This finding may explain why *N. cataria* leaf extract in olive oil enhances or synergizes the repellent effect [24].

Table 2. Molecular docking of nepetalactones and DEET ligands with *Agam*OBP, *Cqui*OBP, and *Aaeg*OBP receptors. The lowest binding energy (kJ/mol) in terms of Vina scores and putative cavity size obtained from CB-Dock2 server.

OBPs	Cavity size (Å³)	DEET	*cis,cis*-NL	*cis-trans*-NL	NL
*Agam*OBP	1159	−6.4	−6.6	−6.6	−6.6
*Cqui*OBP	1643	−6.3	−6.6	−6.7	−6.5
*Aaeg*OBP	1284	−6.2	−7.0	−6.7	−7.0

The binding interactions of DEET and the three nepetalactones with the three OBP receptors were characterized by a combination of hydrophobic contacts, hydrogen bonds, van der Waals forces, π–π stacking, π–σ, and alkyl interactions. For *Agam*OBP, DEET established multiple hydrophobic contacts (alkyl and π–alkyl) with residues Leu73, Ala88, and Met89, as well as van der Waals interactions with Leu80, Glu74, and Gly92. The aromatic ring of DEET formed a key π–π stacking interaction with Trp114, suggesting a central role of this residue in ligand stabilization. *Cis,cis*-NL exhibited strong van der Waals interactions with Gly92, Lys93, Cys95, and Leu96, together with hydrophobic contacts involving Leu73, Leu76, Met89, and Trp114, closely resembling DEET's binding profile. This overlap suggests competitive occupancy of the same binding pocket [18]. Notably, *cis,trans*-NL introduced an additional conventional hydrogen bond and π–σ with Trp114, along with hydrophobic interactions (Leu73, Leu76, His77, Met89) and van der Waals contacts (Leu80, Gly92, Lys93, Cys95, Leu110), thereby enhancing cavity stabilization. Nepetalactone displayed extensive hydrophobic contacts with Leu76, His77, Ala88, Met89, and Trp114, supplemented by van der Waals interactions with Glu74, Leu80, and Gly92, maintaining a pocket occupancy profile similar to DEET (Figure 3). In *Cqui*OBP, DEET bound primarily via hydrophobic

 doi:10.20944/preprints202509.1531.v1

interactions with Leu76, His77, Leu80, Ala88, Met91, Tyr122, and Phe123, along with van der Waals interactions with Tyr10, Leu73, Ile87, Gly92, and His121. A crucial π–π stacking interaction with Trp114 was also observed. *Cis,cis*-NL interacted via van der Waals forces (Tyr10, Leu15, Leu76, Gly92, His111) and hydrophobic contacts (Leu80, Ala88, Met91, Trp114, Phe123). *Cis,trans*-NL retained interactions with residues common to DEET (Leu76, Leu80, Trp114) while introducing additional contacts with His77 and Leu73. However, unfavorable steric clashes were detected, including a bump with Ala88 and a sulfur–X interaction with Met91, suggesting possible strain in this binding pose. Nepetalactone showed a strong π–lone pair interaction with Trp114 and a sulfur–X contact with Met91, in addition to van der Waals interactions with Leu73, Met84, Met89, Gly92, and Tyr122. Hydrophobic contacts with His77, Leu80, and Ala88 further supported stable insertion into the binding cavity (Figure 4). For *Aaeg*OBP, DEET engaged a dense hydrophobic network involving Leu76, Ala88, Met91, and Tyr123, closely resembling its binding in *Cqui*OBP. Additional van der Waals interactions were formed with Phe15, Gly92, Phe123, and Leu124. A π–π stacking interaction with Trp114 was again identified as a key stabilizing feature. *Cis,cis*-NL displayed a similar interaction pattern, suggesting that it mimics DEET's binding mode, with additional π–σ and sulfur–X interactions involving Trp114 and Met91, respectively. *Cis-trans*-NL formed stabilizing contacts with His111, while Trp114 engaged in a critical π–σ interaction. NL exhibited the broadest interaction network, with van der Waals contacts (Leu76, Leu80, Gly92, His125) and hydrophobic interactions (Phe15, Ala88, Met91, Trp114, Phe123), highlighting its strong cavity occupancy and stabilization potential (Figure 5).

Hence, these interaction profiles indicate that nepetalactones, establish more diverse and stabilizing contacts than DEET, often involving the conserved Trp114 residue. This suggests that nepetalactones may achieve stronger and more specific stabilization within the OBP binding pockets, supporting their potential as effective bio-repellent ligands.

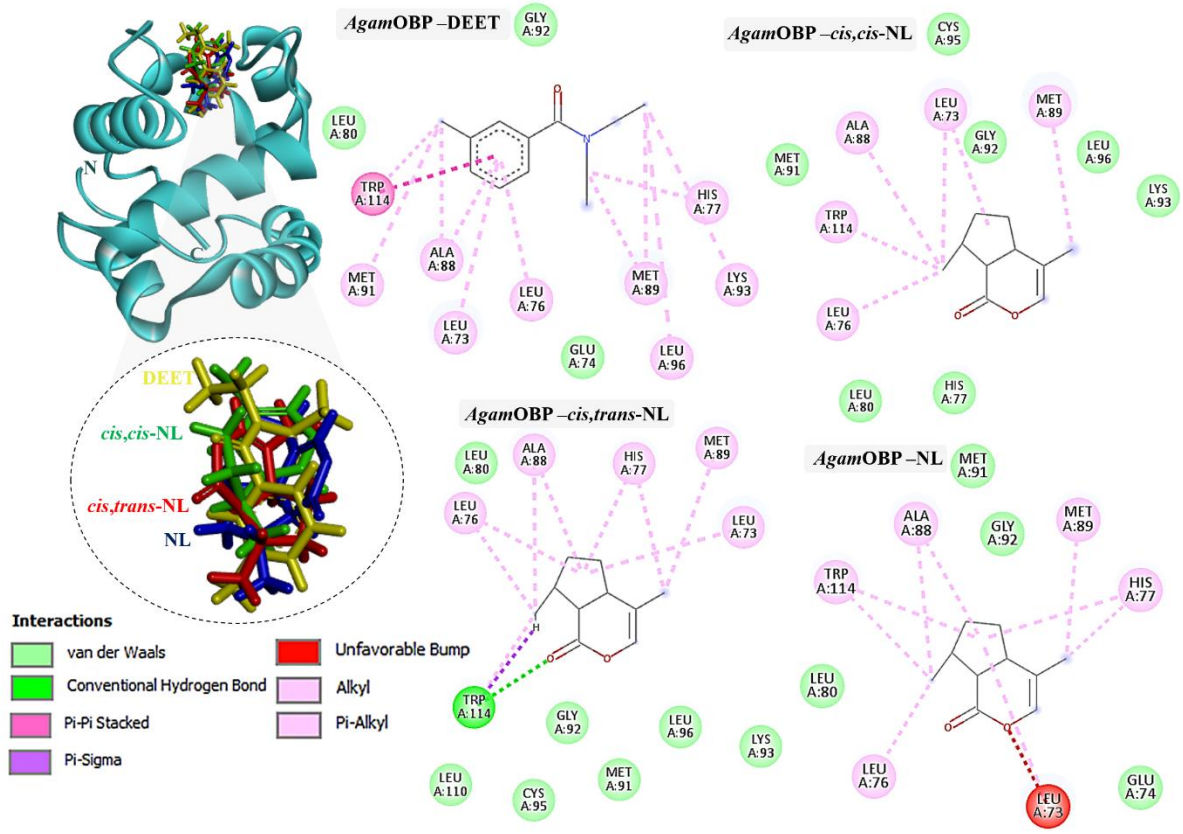

Figure 3. Complexes of *Agam*OBP with DEET, *cis,cis*-NL, *cis,trans*-NL, and NL are represented in yellow, green, red, and blue sticks, respectively. The dotted circles highlight the magnified superimposition of DEET and

 doi:10.20944/preprints202509.1531.v1

nepetalactone ligands after docking. The right panel shows the 2D schematic interaction diagrams of each complex.

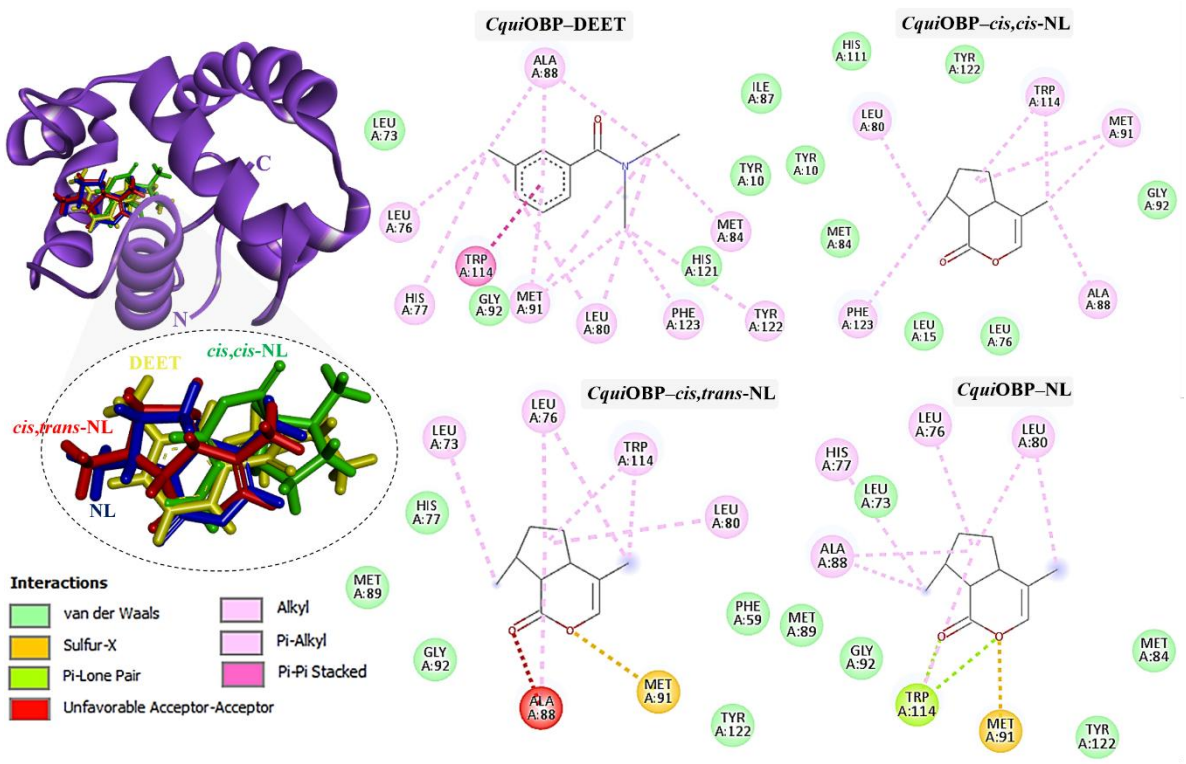

Figure 4. Complexes of *Cqui*OBP with DEET, *cis,cis*-NL, *cis,trans*-NL, and NL are represented in yellow, green, red, and blue sticks, respectively. The dotted circles highlight the magnified superimposition of DEET and nepetalactone ligands after docking. The right panel shows the 2D schematic interaction diagrams of each complex.

 doi:10.20944/preprints202509.1531.v1

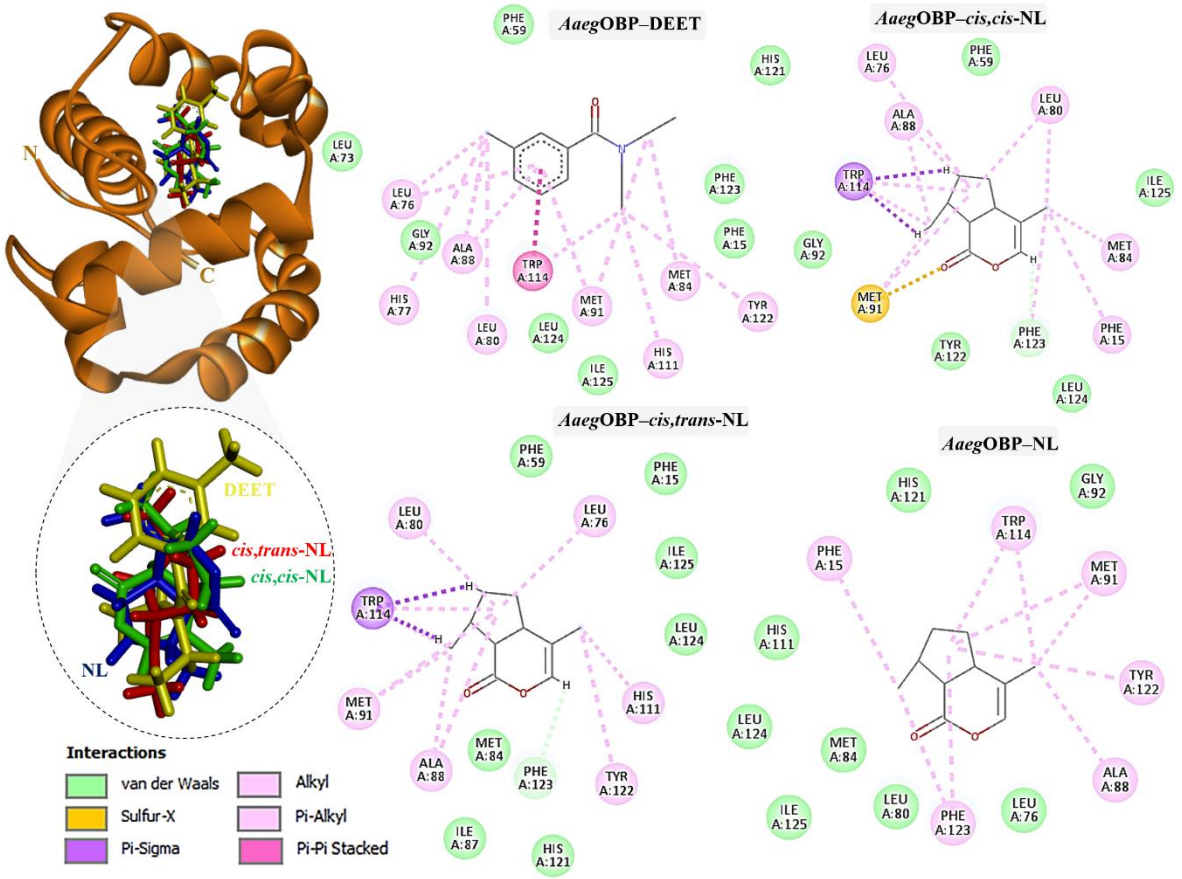

Figure 5. Complexes of *Aaeg*OBP with DEET, *cis,cis*-NL, *cis,trans*-NL, and NL are represented in yellow, green, red, and blue sticks, respectively. The dotted circles highlight the magnified superimposition of DEET and nepetalactone ligands after docking. The right panel shows the 2D schematic interaction diagrams of each complex.

2.4. Molecular Dynamics Simulations Analysis

Molecular dynamics simulations were performed to evaluate the binding stability and conformational dynamics of DEET, cis,cis-NL, cis-trans-NL, and NL with the three OBP isoforms. Binding free energy, root-mean-square deviation (RMSD), root-mean-square fluctuation (RMSF), solvent-accessible surface area (SASA), and radius of gyration (Rg) were assessed to characterize the stability and conformational behavior of the ligand–protein complexes (Table 3) [27,28].

All ligands demonstrated favorable binding free energies, confirming their ability to stably associate with OBP receptors. DEET, used as the reference ligand, exhibited consistently strong binding energies with AgamOBP (−9123.22 kcal/mol), CquiOBP (−9002.12 kcal/mol), and AaegOBP (−9090.19 kcal/mol), reaffirming its established role as a broad-spectrum synthetic repellent. Notably, cis,cis-NL displayed even stronger binding to AgamOBP (−9130.37 kcal/mol) compared to DEET, along with high affinity for AaegOBP (−9082.88 kcal/mol) and CquiOBP (−8990.80 kcal/mol). This suggests that cis,cis-NL may act as a competitive or alternative bio-repellent to DEET, particularly in An. gambiae. Similarly, cis-trans-NL exhibited stronger binding to AaegOBP (−9095.99 kcal/mol) and AgamOBP (−9120.15 kcal/mol) than DEET, while its interaction with CquiOBP (−8996.77 kcal/mol) was only slightly lower, approaching the binding energy of DEET. NL demonstrated its strongest binding to AaegOBP (−9087.10 kcal/mol), followed by CquiOBP (−8999.34 kcal/mol), both comparable to DEET. The overall similarity in binding energies across the three OBPs indicates conserved ligand–protein recognition, although subtle variations among isoforms point to species-dependent preferences in ligand accommodation. These MD results collectively suggest that nepetalactones can achieve binding stability and energetics comparable to DEET across multiple mosquito OBPs, highlighting their potential as natural alternatives to synthetic repellents.

 doi:10.20944/preprints202509.1531.v1

The molecular dynamics simulations confirmed that all OBP–ligand complexes attained structural stability throughout the trajectory. RMSD values for all complexes were consistently within the range of 0.13–0.20 nm, indicating stable protein–ligand conformations. Interestingly, DEET–OBP complexes exhibited slightly lower RMSD values (0.13–0.17 nm) compared to the nepetalactones, suggesting stronger conformational stability. However, the cis-trans-NL–AgamOBP complex displayed higher stability (0.15 nm) than DEET, while NL binding to AaegOBP showed comparable stability to DEET. In addition, RMSF values revealed limited residue flexibility, ranging from 0.26 to 0.60 nm across all systems. DEET complexes demonstrated narrower fluctuation ranges (0.27–0.43 nm), reflecting greater rigidity of the protein backbone upon DEET binding. In contrast, nepetalactones induced higher fluctuations in AaegOBP, while cis-trans-NL also increased structural fluctuations in CquiOBP compared to DEET (Figure 6). These observations suggest that although nepetalactones bind effectively, they tend to introduce slightly greater local flexibility within the binding pocket, which could influence ligand-induced conformational dynamics and odorant recognition.

The solvent-accessible surface area values remained stable across all complexes, ranging between 75.02–78.87 nm². DEET-bound complexes generally showed slightly higher SASA values (77.00–78.87 nm²), implying that DEET binding exposes a marginally larger protein surface. By contrast, the cis,cis-NL–AgamOBP complex exhibited the lowest SASA (75.02 nm²), indicating a more compact ligand–protein interface and suggesting stronger encapsulation of the ligand within the binding pocket. Finally, the radius of gyration (Rg) values were highly consistent across all systems (1.38–1.40 nm), confirming that ligand binding did not significantly affect the overall compactness of the OBP structures (Figure 7). Therefore, these findings indicate that both DEET and nepetalactones stabilize OBPs without inducing major conformational rearrangements, although subtle differences in local flexibility and solvent exposure distinguish the binding behavior of these ligands.

Table 3. Analysis of binding free energy ($\Delta G_{MM\text{-}PBSA}$), RMSD, RMSF, SASA, and radius of gyration of OBP–ligand complexes after a 100 ns simulation.

Compound	OBPs	$\Delta G_{MM\text{-}PBSA}$ (kcal/mol)	RMSD (nm)	RMSF (nm)	SASA (nm²)	gyration (nm)
DEET	*Agam*OBP	−9123.22	0.17	0.43–0.05	78.87	1.40
	*Cqui*OBP	−9002.52	0.14	0.34–0.05	77.68	1.39
	*Aaeg*OBP	−9090.19	0.13	0.27–0.05	77.00	1.39
cis,cis-NL	*Agam*OBP	−9130.37	0.18	0.26–0.05	75.02	1.38
	*Cqui*OBP	−8990.80	0.17	0.36–0.06	77.24	1.39
	*Aaeg*OBP	−9082.88	0.18	0.60–0.06	76.98	1.39
cis-trans-NL	*Agam*OBP	−9120.15	0.15	0.35–0.05	77.76	1.40
	*Cqui*OBP	−8996.77	0.15	0.32–0.06	76.62	1.40
	*Aaeg*OBP	−9095.99	0.19	0.40–0.05	78.13	1.40
NL	*Agam*OBP	−9115.51	0.2	0.34–0.05	76.13	1.39
	*Cqui*OBP	−8999.34	0.15	0.28–0.05	76.78	1.39
	*Aaeg*OBP	−9087.15	0.13	0.41–0.05	76.61	1.39

$\Delta G_{MM\text{-}PBSA}$ was calculated from the terms above (ΔG_{gas} + ΔG_{sol}). Total gas phase energy (ΔG_{gas}) consists of the electrostatic energy (ΔG_{ele}) and the van der Waals energy (ΔG_{vdW}), which are significant for binding. Total solvation energy (ΔG_{sol}) consists of non-polar solvation energy (ΔG_{np}) and polar solvation energy (ΔG_{pb}).

 doi:10.20944/preprints202509.1531.v1

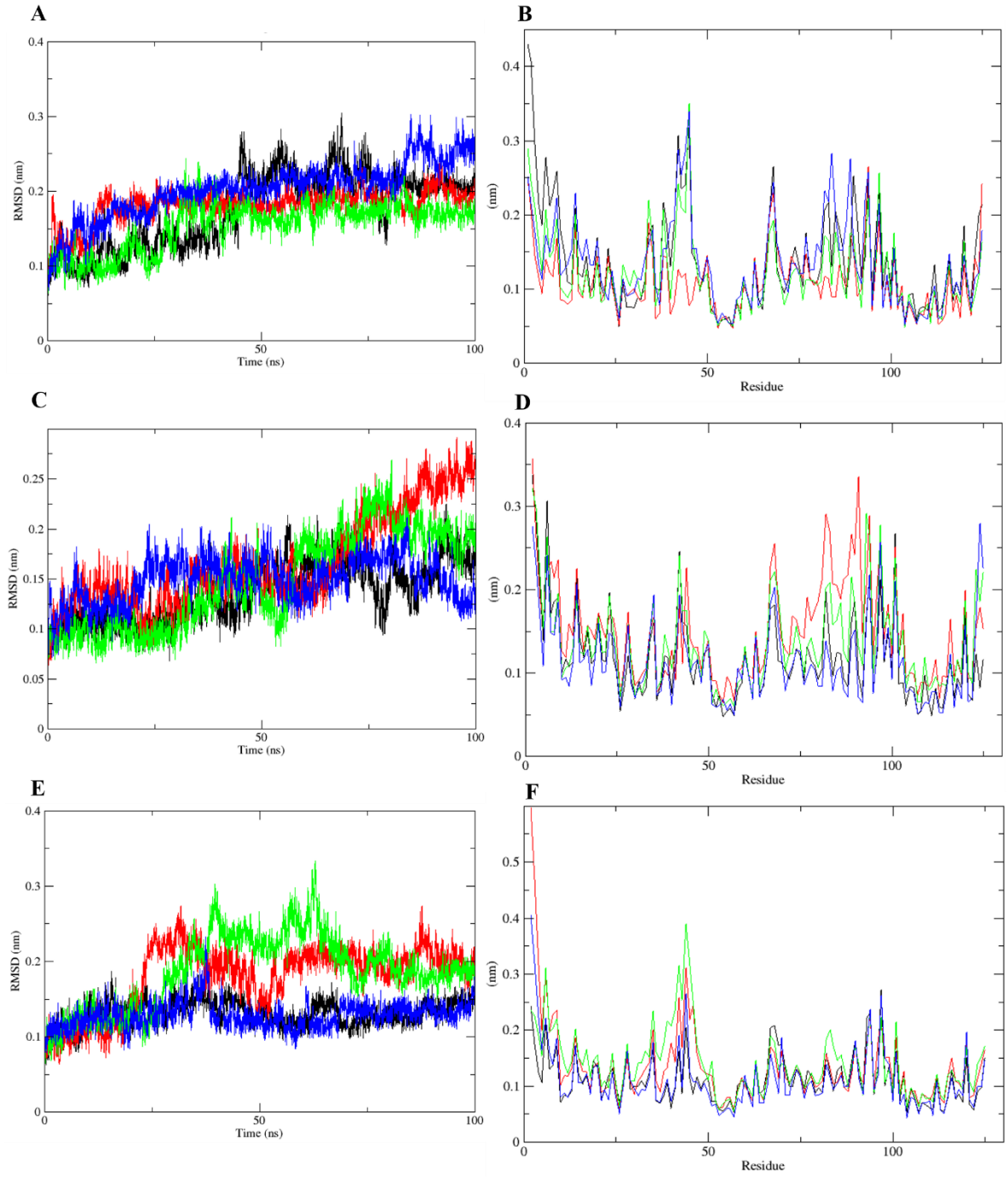

Figure 6. Root-mean-square deviation (RMSD) and root-mean-square fluctuation (RMSF) of AgamOBP **(A, B)**, CquiOBP **(C, D)**, and AaegOBP **(E, F)** complexes with DEET, cis,cis-nepetalactone, cis,trans-nepetalactone, and nepetalactone, represented by black, red, green, and blue lines, respectively.

 doi:10.20944/preprints202509.1531.v1

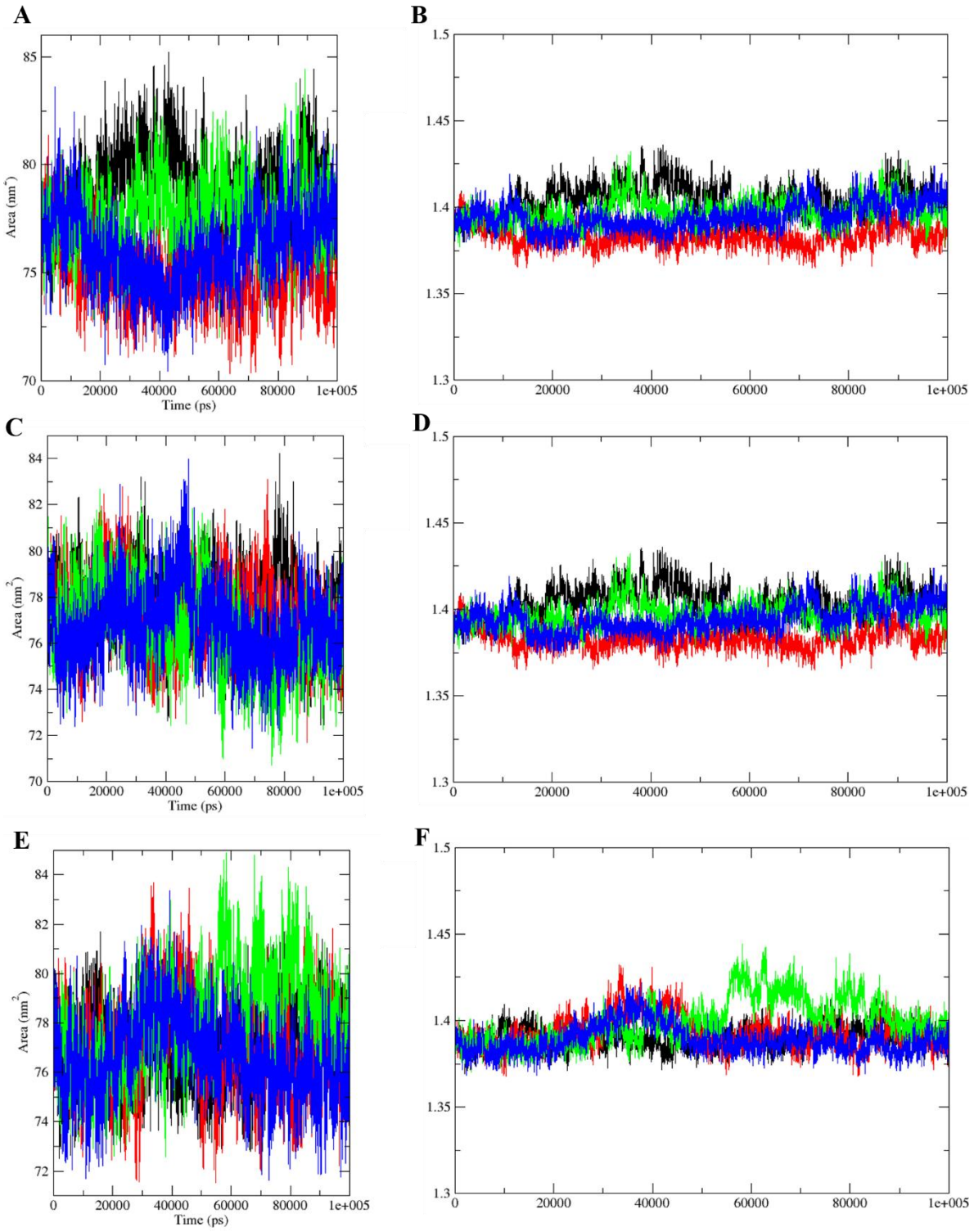

Figure 7. Time evolution of the radius of gyration (Rg) and solvent-accessible surface area (SASA) of AgamOBP **(A, B)**, CquiOBP **(C, D)**, and AaegOBP **(E, F)** complexes with DEET, cis,cis-nepetalactone, cis,trans-nepetalactone, and nepetalactone, represented by black, red, green, and blue lines, respectively.

2.5. ADMET Analysis

ADMET profiling supported the potential of cis,cis-NL, cis,trans-NL, and NL as safe, plant-based bio-repellents (Table 4) [29]. Cis,cis-NL showed markedly higher water solubility than DEET and other nepetalactones, suggesting enhanced formulation potential. Skin permeability was consistently low, including −2.282, −2.212, −2.212 log Kp), implying reduced dermal penetration and greater safety compared to DEET. Distribution was minimal, with cis,cis-NL showing the highest plasma availability. Moderate BBB penetration was observed, though CNS permeability remained

 doi:10.20944/preprints202509.1531.v1

low, minimizing neurological risk. None were CYP3A4 or CYP2D6 substrates; only DEET and cis,cis-NL inhibited CYP1A2. Clearance was highest for cis,cis-NL, followed by DEET and other isomers. Toxicological predictions indicated low mutagenicity risk. Interestingly, skin sensitization was predicted for DEET and the nepetalactone isomers, but not for cis,cis-NL. Overall, cis,cis-NL followed by other isoforms demonstrated superior safety, solubility, clearance, and environmental compatibility, highlighting it as the most promising bio-repellent candidate relative to DEET.

Table 4. The ADMET properties of cis,cis-NL, cis,trans-NL, and NL compared to DEET using pkCSM pharmacokinetics server.

Property	Model Name	Predicted Value	*Cis-cis*-NL	*Cis-trans*-NL	NL	Unit
Absorption	Water solubility	−2.65	−0.10	−2.52	−2.52	Numeric (log mol/L)
Absorption	Skin Permeability	−2.67	−2.28	−2.21	−2.21	Numeric (log Kp)
Absorption	P-glycoprotein substrate	No	No	No	No	Categorical (Yes/No)
Absorption	P-glycoprotein I & II inhibitor	No	No	No	No	Categorical (Yes/No)
Distribution	VDss (human)	0.16	0.28	0.19	0.19	Numeric (log L/kg)
Distribution	BBB permeability	0.36	0.29	0.70	0.70	Numeric (log BB)
Distribution	CNS permeability	−1.93	−2.83	−2.08	−2.08	Numeric (log PS)
Metabolism	CYP2D6 and CYP3A4 substrate	No	No	No	No	Categorical (Yes/No)
Metabolism	CYP1A2 inhibitor	Yes	Yes	No	No	Categorical (Yes/No)
Metabolism	CYP2C9, CYP2D6 and CYP3A4 inhibitor	No	No	No	No	Categorical (Yes/No)
Excretion	Total Clearance	0.59	0.91	0.11	0.11	Numeric (log ml/min/kg)
Excretion	Renal OCT2 substrate	No	No	No	No	Categorical (Yes/No)
Toxicity	hERG I & II inhibitor	No	No	No	No	Categorical (Yes/No)
Toxicity	Oral Rat Acute Toxicity (LD_{50})	2.31	2.48	1.77	1.77	Numeric (mol/kg)
Toxicity	Oral Rat Chronic Toxicity (LOAEL)	1.46	4.57	2.30	2.30	Numeric (log mg/kg_bw/day)
Toxicity	Hepatotoxicity	No	No	No	No	Categorical (Yes/No)
Toxicity	Skin Sensitisation	Yes	No	Yes	Yes	Categorical (Yes/No)

 doi:10.20944/preprints202509.1531.v1

Toxicity	*T.Pyriformis* toxicity	0.59	−0.96	0.23	0.23	Numeric (log μg/L)
Toxicity	Minnow toxicity	1.19	4.81	1.30	1.30	Numeric (log mM)

3. Discussion

The present study integrated phytochemical characterization, molecular docking, molecular dynamics simulations, and ADMET profiling to systematically evaluate nepetalactone and its derivatives from *N. cataria* in comparison with DEET, the widely used active ingredient in commercial insect repellents [5,11]. Despite its efficacy, DEET has been associated with adverse neurological, cardiovascular, dermatological, and gastrointestinal effects, particularly in children, following ingestion or excessive dermal exposure [30]. By employing a multifaceted approach, this study not only elucidated the molecular determinants of repellent activity and the conformational dynamics of mosquito odorant-binding proteins (OBPs), but also assessed the pharmacokinetic and toxicological profiles of nepetalactones. Collectively, these findings provide a strong rationale for the development of nepetalactone-based bio-repellents as safer and more environmentally sustainable alternatives to DEET.

For phytochemical characterization, GC–MS/MS analysis highlighted the dominance of iridoid lactones, including *cis-cis*-NL, *cis,trans*-NL, and NL in extracts obtained via dried leaf oil extraction (DOE) and stream distillation (SDE). The most notable outcome of this study was the detection of *cis-trans*-NL (4.89%), *cis,cis*-NL (1.80%), and NL (0.23%) exclusively in the dried leaf oil extract. SDE fraction included *cis,trans*-NL (52.80%) and *cis,cis*-NL (47.20%) as dominant compositions. These bicyclic iridoid lactones are well established as the key insect-repellent constituents of *N. cataria*. While originally described as feline attractants [31], subsequent studies confirmed their potent repellency against Aedes, Culex, and Anopheles [32,33]. Mechanistically, nepetalactones interact with odorant-binding proteins (OBPs) and olfactory receptors involved in host-seeking, particularly OR2 and OR8, which respond to human kairomones such as octenol and lactic acid [34,35]. By misactivating these pathways, they mimic DEET's sensory disruption mechanism. Interestingly, both fresh and dried leaf extracts (FOE and DOE) contained alkanes such as undecane, 2-Methyldecahydronaphthalene, and 2,6,10-Trimethyldodecane, which were primarily derived from the olive oil used as the extraction solvent. Though less bioactive than iridoids, hydrocarbons may indirectly enhance repellency by modulating volatility and prolonging release of active compounds [22,24,36]. Structural similarity of branched alkanes to mosquito cuticular hydrocarbons may also create olfactory interference [37]. Thus, hydrocarbons likely act as synergists that stabilize and extend nepetalactone activity. Moreover, FOE and DOE extracts were enriched in alcohols (e.g., 2-Hexyl-1-octanol) and esters (e.g., tetrahydrogeranyl formate), which was found in olive oil (Table 1) [38]. These moderately volatile compounds can disrupt host-seeking either by masking attractant cues or activating deterrent receptors [39]. Esters, in particular, may function as repellent enhancers. Butylated hydroxytoluene (BHT), the major compound detected in both maceration extracts, likely functions as a natural antioxidant that stabilizes iridoids and may also act as a mild deterrent [40,41]. Dried extracts also contained 1,3-di-tert-butylbenzene (4.70%), an aromatic hydrocarbon with insect-deterrent properties. Interestingly, mixtures of hydrocarbons with iridoids may result in prolonging the effectiveness of long-acting lactone repellents [14,15]. Moreover, these stabilizing agents may not only preserve bioactivity but also contribute synergistically to repellency. Thus, these findings corroborate previous reports indicating that nepetalactone-rich dried extracts possess repellent activity comparable to DEET [11,32]. Notably, DOE maceration represents a simple and eco-friendly extraction approach, potentially enhanced by synergistic contributions from hydrocarbons, oxygenated volatiles, and phenolic compounds. In contrast, SDE yielded the highest concentrations of nepetalactone.

Docking studies demonstrated that all nepetalactone isomers exhibited stronger binding affinities than DEET across the three mosquito OBPs (*Agam*OBP, *Cqui*OBP, and *Aaeg*OBP). A

 doi:10.20944/preprints202509.1531.v1

conserved Trp114 residue consistently stabilized ligand binding via π–π and hydrophobic interactions, underscoring its critical role in odorant recognition [18] (Lagarde et al., 2011; Zhou et al., 2008). Among the isomers, *cis,trans*-NL established the most extensive interaction network, engaging in hydrogen bonding and π–σ interactions with Trp114 in *Agam*OBP, while both *cis,cis*- and *cis,trans*-NL were further stabilized through π–σ interactions with Trp114 of *Aaeg*OBP. Functionally, this is consistent with the known function of OBPs that they solubilize hydrophobic odorants and deliver them to olfactory receptors. In contrast, DEET is thought to disrupt this process by binding OBPs with high affinity, thereby preventing recognition of natural attractants [42]. Similarly, nepetalactones form stable hydrophobic and hydrogen-bonding interactions within OBP binding cavities, promoting conformational rigidity [43]. OBPs are characterized by broad ligand specificity, and ligands that engage multiple residues are more likely to alter protein conformational dynamics [44,45]. Such expanded binding footprints may explain the superior binding affinity and potentially enhanced olfactory disruption exhibited by nepetalactones compared to DEET. Additionally, the results suggest that *N. cataria* leaf extract in olive oil may exert an enhanced or synergistic repellent effect, owing to the presence of ligands with binding affinities to mosquito OBPs comparable to or greater than that of DEET. The strong interactions observed for both nepetalactones and these additional ligands reinforce their roles as key bioactive constituents. Collectively, these findings underscore the potential of *N. cataria*-derived compounds, either individually or in combination with carrier oils, as natural alternatives to synthetic repellents.

The molecular dynamics simulations provided critical insights into the conformational behavior of three OBP receptors upon ligand binding, offering mechanistic evidence for the stability and potential efficacy of nepetalactone and derivatives compared to the benchmark repellent DEET. The consistently low RMSD values (0.13–0.20 nm) across all OBP–ligand complexes confirmed that binding did not disrupt the global protein architecture, indicating that nepetalactone isomers are well accommodated within the conserved binding pockets. Such stability is essential for ligand recognition and transport, as OBPs must maintain structural integrity while transiently interacting with semiochemicals [28,46]. Specifically, the *cis,trans*-NL–*Agam*OBP complex demonstrated higher stability (0.15 nm) than DEET, suggesting that this isomer can form an equally, if not more, stable interaction within the *Anopheles gambiae* OBP binding pocket. Such stability may reflect more extensive or complementary residue–ligand contacts, consistent with docking predictions that nepetalactones engage broader interaction networks compared to DEET. Equally important is the finding that nepetalactone binding to *Aaeg*OBP yielded stability comparable to DEET, underscoring the potential cross-species effectiveness of nepetalactones. Since *Aedes aegypti* is a major vector for arboviruses such as dengue, chikungunya, and Zika, the ability of nepetalactones to maintain stable interactions with *Aaeg*OBP receptor is a promising indicator of their applied utility. Furthermore, nepetalactones induced higher RMSF fluctuations at key loop regions surrounding the binding pocket. This localized flexibility is critical, as ligand-induced conformational dynamics have been implicated in OBP-mediated odorant release and receptor activation [47,48]. Interestingly, *cis,cis*-NL–*Agam*OBP complexes exhibited reduced SASA, suggesting a more encapsulated ligand conformation. Such tight binding could reduce the accessibility of competing host odorants, thereby enhancing repellent efficacy. By contrast, *cis-trans*-NL promoted slightly higher flexibility in *Aaeg*OBP, suggesting potential differences in species-specific repellency efficacy. These findings resonate with behavioral studies showing that nepetalactone isomers vary in repellency strength depending on the mosquito species targeted. Thus, while DEET stabilizes OBPs in a more rigid conformation, nepetalactones appear to exploit structural adaptability, inducing conformational shifts that may interfere with the precise odorant recognition and transport essential for host-seeking behavior. This dual mechanism, effective binding combined with dynamic disruption, represents a novel pathway for repellent function.

ADMET predictions indicated that nepetalactones possess favorable pharmacokinetic and safety profiles compared to DEET. Importantly, all nepetalactones have low skin permeability, indicating greater safety compared to DEET. None of the ligands were predicted as substrates or inhibitors of

 doi:10.20944/preprints202509.1531.v1

major CYP450 isoforms (except for CYP1A2 inhibition by DEET and *cis,cis*-NL), suggesting a lower risk of metabolic interference. From a toxicological perspective, DEET was associated with skin sensitization and neurological concerns [50,51]. In contrast, *cis,cis*-NL showed a more benign profile, lacking skin sensitization alerts and hepatotoxicity predictions, while retaining strong binding to mosquito OBPs. Overall, the in silico evidence supports its safer use profile.

The combined evidence suggests that nepetalactone isomers represent strong candidates for bio-repellent development. Their ability to bind deeply and flexibly to OBPs, combined with favorable ADMET properties, provides a rational basis for their efficacy and safety compared to DEET. Importantly, the plant-derived nature of nepetalactones ensures ecological sustainability, aligning with the growing demand for natural and environmentally compatible repellents. Future studies should integrate electrophysiological assays to validate OBP-mediated disruption, as well as behavioral bioassays against different mosquito species. Additionally, formulation strategies should exploit the volatility of nepetalactones while ensuring stability for long-term protection in field conditions.

4. Materials and Methods

4.1. Preparation of Nepeta Cataria Leaf Extraction

4.1.1. Extraction via Steam Distillation

To maximize the yield of repellent compounds from catnip (Nepeta cataria), nepetalactone was extracted by steam distillation. A total of 100 g of dried leaf was suspended in 2.5 L of distilled water and subjected to distillation in a stainless-steel apparatus for 8 h, boiling. The hydrosol fraction was collected and stored in a tightly sealed container at 4 °C for further use [20,52,53].

4.1.2. Extraction by the Maceration Method Using Olive Oil Solvent

Both fresh and dried catnip leaves were used. For dried samples, leaves were cut into small pieces and dried in a hot-air oven at 45 °C for 8 h to remove moisture. Fresh leaves were cut into small pieces without prior drying. Each sample was macerated in olive oil at a 1:10 (w/v) ratio (sample: olive oil), using the same raw material weight for both fresh and dried samples. The mixtures were incubated at 90 °C for 2 h with intermittent stirring to facilitate extraction. The extracts were filtered through a muslin cloth (100–400 mesh; approximate pore size 37–149 μm) to remove coarse plant debris. The filtrates were collected and stored at 4 °C in a tightly sealed container until further analysis.

4.2. Identification of Chemical Compositions by Using GC-MS/MS

After extraction, 4 mL of catnip extract was mixed with 2 mL of hexane. Then, 0.4 mL of 0.9% NaCl solution and anhydrous $MgSO_4$ powder were added to remove residual water from the sample. From the mixture, the hexane layer (upper phase) was transferred into a clean vial and evaporated under a gentle stream of nitrogen gas. The concentrated residue was re-dissolved in 1 mL of diethyl ether. A 2 μL aliquot of the prepared sample was injected into the GC–MS/MS system. The analysis was performed using a Trace 1610 system equipped with a TG-5MS capillary column (30 m × 0.25 mm i.d., 0.25 μm film thickness) (Thermo Scientific, United States). Helium was used as the carrier gas at a constant flow rate of 1 mL/min. The oven temperature program was set to an initial temperature of 70 °C, increased at 2 °C/min to 170 °C, and then further increased at 5 °C/min to 230 °C. Electron impact (EI) ionization was employed at 50 eV. The total run time was 63 minutes. TSQ 9610 Triple quadrupole mass spectrometer (Thermo Scientific, United States) was used as a detector. The mass spectra were identified by comparison with the NIST 2020 mass spectral library (USA), and compounds from the catnip leaf extract that showed a match of more than 70% with the library were selected [53].

 doi:10.20944/preprints202509.1531.v1

4.3. Structural Analysis and Comparison of AgamOBP, CquiOBP, and AaegOBP

The experimental protein models analyzed were Odorant-Binding Proteins (OBPs). Three OBPs were selected, including CquiOBP1 from Culex quinquefasciatus (PDB ID: 3OGN), AaegOBP1 from Aedes aegypti (PDB ID: 3K1E, chain A), and AgamOBP1 from Anopheles gambiae (PDB ID: 3N7H) [42,54,55]. The 3D structures were retrieved in PDB format from the RCSB Protein Data Bank (https://www.rcsb.org/, accessed on 30 June 2025) and were virtualized by using Discovery Studio (version 2024). All OBPs sequences were aligned on Clustal Omega (https://www.ebi.ac.uk/jdispatcher/msa/clustalo? stype=protein, accessed on 1 July 2025). The conserved amino acids were generated with Multiple Align Show (https://www.bioinformatics.org/sms/multi_align.html, accessed on 1 July 2025).

4.4. Molecular Docking of N. cataria Phytochemicals with the OBP Receptors

All 3D structures of OBPs and the selected ligands used, with their SDF structures obtained from PubChem (https://pubchem.ncbi.nlm.nih.gov/, accessed on 2 July 2025). Molecular docking was performed using CB-Dock2 (https://cadd.labshare.cn/cb-dock2/ index.php, accessed on 5 July 2025), which provided binding cavity parameters (Å) [26]. The resulting protein–ligand complexes were visualized and analyzed with Discovery Studio (version 2024).

4.5. Molecular Dynamics Simulations and Analysis

Molecular dynamics simulations were performed to investigate the interactions between *Agam*OBP, *Cqui*OBP, and *Aaeg*OBP receptors and three nepetalactone isoforms as ligands. All simulations were conducted using GROMACS 5.1.4 with the OPLS/AA force field. Each system was solvated in an orthorhombic box filled with TIP3P water molecules, and counterions (Na^+ and Cl^-) were added to neutralize the system and achieve a physiological salt concentration of 0.15 M. Energy minimization was followed by equilibration under NVT and NPT ensembles. Temperature was maintained at 300 K using the Nosé–Hoover thermostat, and pressure was controlled at 1.0 bar with the Martyna–Tobias–Klein barostat. Production simulations were run for 100 ns, with trajectories recorded every 20 ps, yielding 5001 frames for analysis [56].

Trajectory analyses included calculation of structural parameters such as root mean square deviation (RMSD), root mean square fluctuation (RMSF), solvent-accessible surface area values (SASA), and gyration (gy). Binding free energies ($\Delta G_{MM\text{-}PBSA}$) were estimated using the g_mmpbsa tool, which applies the molecular mechanics Poisson–Boltzmann surface area (MM-PBSA) method within GROMACS [49,57]. Graphical analyses were performed using QtGrace (version 0.2.6).

4.6. ADMET Analysis

To evaluate safety, the pharmacokinetics and toxicity of nepetalactone and its isomers, compared to DEET, were predicted using the pkCSM pharmacokinetics server (https://biosig.lab.uq.edu.au/pkcsm/prediction, accessed on 29 June 2025). Canonical SMILES for each compound were obtained from PubChem and submitted for ADMET (Absorption, Distribution, Metabolism, Excretion, and Toxicity) analysis. Predicted parameters included solubility, P-glycoprotein interactions, and skin permeability. Distribution properties assessed volume of distribution, plasma protein binding, blood–brain barrier penetration, and CNS access. Metabolism was evaluated through cytochrome P450 inhibition and substrate predictions. Excretion was estimated via renal clearance and OCT2 substrate status. Toxicity profiles included human and animal systemic toxicity, hepatotoxicity, skin sensititation, cardiotoxicity, and ecotoxicity [29]. This computational assessment was applied since repellents, though topically used, can penetrate skin and cause systemic or local toxicity, as reported for DEET [18].

5. Conclusions

This study integrated phytochemical analysis, molecular docking, molecular dynamics simulations, and ADMET profiling to comprehensively evaluate nepetalactone isomers from *N.*

 doi:10.20944/preprints202509.1531.v1

cataria in comparison with DEET. GC–MS/MS confirmed nepetalactones as dominant constituents in steam distillation fractions followed by dried leaf extracts, corroborating their established role as key insect-repellent compounds. Additional constituents, including hydrocarbons, alcohols, esters, and antioxidants present in maceration extracts, may synergistically enhance repellent efficacy and stability. Docking and dynamics simulations revealed that nepetalactones exhibit stronger and more extensive interactions with mosquito OBPs than DEET, particularly through conserved residues such as Trp114. These interactions were accompanied by favorable conformational stability and localized flexibility, suggesting dual mechanisms of action: strong binding and disruption of odorant recognition. ADMET predictions further highlighted the safety advantages of nepetalactones, contrasting with DEET's reported neurological and dermatological concerns. Collectively, these findings underscore the potential of nepetalactone-based formulations as safe, effective, and environmentally sustainable alternatives to synthetic repellents. Further study, we will combine electrophysiological validation with behavioral bioassays across mosquito species, alongside optimized formulation strategies to balance volatility and long-term stability for practical field applications.

Supplementary Materials: The following supporting information can be downloaded at the website of this paper posted on Preprints.org.

Author Contributions: Conceptualization, N.K. and S.N.; methodology, S.N., T.K., J.C. and S.S.; software, S.N. and P.J.; validation and formal analysis, N.K., S.N., J.S. and S.Du.; resources, N.K., S.Du., P.A. and S.S.; data curation, N.K., S.N., J.S. and S.Da.; writing—original draft preparation, S.N. and T.K.; writing—review and editing, N.K., S.N., J.S. and P.S.; visualization, S.N.; supervision, N.K. and S.N.; project administration, N.K.; funding acquisition, N.K., S.D. and S.S. All authors have read and agreed to the published version of the manuscript.

Funding: This work was supported by the Thailand Science Research and Innovation Fundamental Fund, fiscal year 2025.

Institutional Review Board Statement: Not applicable.

Informed Consent Statement: Not applicable.

Data Availability Statement: The original contributions presented in this study are included in this article. Further inquiries can be directed to the corresponding author.

Acknowledgments: The authors are grateful to the Research Center and Central Laboratory, Faculty of Agriculture, Khon Kaen University, Khon Kaen, Thailand to provide facilities in GC-MS/MS instrument and analysis.

Conflicts of Interest: The authors declare no conflicts of interest.

Abbreviations

The following abbreviations are used in this manuscript:

DEET	N,N-diethyl-meta-toluamide
TRPA1	Transient receptor potential ankyrin 1
OBP	Odorant-binding protein
GC–MS/MS	Gas chromatography–tandem mass spectrometry
ADMET	Absorption, Distribution, Metabolism, Excretion, and Toxicity
SDE	Stream distillation extraction
FOE	Fresh leaf in olive oil extraction
DOE	Dried leaf in olive oil extraction
NL	Nepetalactone
cis,*cis*-NL	*cis*,*cis*-nepetalactone
cis,*trans*-NL	*cis*,*trans*-nepetalactone

 doi:10.20944/preprints202509.1531.v1

References

1. Onen, H.; Luzala, M. M.; Kigozi, S.; Sikumbili, R. M.; Muanga, C. K.; Zola, E. N.; Wendji, S. N.; Buya, A. B.; Balciunaitiene, A.; Viškelis, J.; Kaddumukasa, M. A.; Memvanga, P. B. Mosquito-Borne Diseases and Their Control Strategies: An Overview Focused on Green Synthesized Plant-Based Metallic Nanoparticles. *Insects* **2023**, *14* (3), 221. https://doi.org/10.3390/insects14030221.
2. Bamou, R.; Mayi, M. P. A.; Djiappi-Tchamen, B.; Nana-Ndjangwo, S. M.; Nchoutpouen, E.; Cornel, A. J.; Awono-Ambene, P.; Parola, P.; Tchuinkam, T.; Antonio-Nkondjio, C. An Update on the Mosquito Fauna and Mosquito-Borne Diseases Distribution in Cameroon. *Parasit. Vectors* **2021**, *14* (1), 527. https://doi.org/10.1186/s13071-021-04950-9.
3. Leal, W. S. The Enigmatic Reception of DEET—The Gold Standard of Insect Repellents. *Curr. Opin. Insect Sci.* **2014**, *6*, 93–98. https://doi.org/10.1016/j.cois.2014.10.007.
4. Rodriguez, S. D.; Drake, L. L.; Price, D. P.; Hammond, J. I.; Hansen, I. A. The Efficacy of Some Commercially Available Insect Repellents for *Aedes aegypti* (Diptera: Culicidae) and *Aedes albopictus* (Diptera: Culicidae). *J. Insect Sci.* **2015**, *15* (1), 140. https://doi.org/10.1093/jisesa/iev125.
5. Chen-Hussey, V.; Behrens, R.; Logan, J. G. Assessment of Methods Used To Determine the Safety of the Topical Insect Repellent N,N-Diethyl-m-Toluamide (DEET). *Parasit. Vectors* **2014**, *7*, 173. https://doi.org/10.1186/1756-3305-7-173.
6. Roy, D. N.; Goswami, R.; Pal, A. The Insect Repellents: A Silent Environmental Chemical Toxicant to the Health. *Environ. Toxicol. Pharmacol.* **2017**, *50*, 91–102. https://doi.org/10.1016/j.etap.2017.01.019.
7. Hazarika, H.; Krishnatreyya, H. Technological Advancements in Mosquito Repellents: Challenges and Opportunities in Plant-Based Repellents. *Acta Parasitol.* **2025**, *70* (3), 117. https://doi.org/10.1007/s11686-025-01054-7.
8. da Costa, K. S.; Galúcio, J. M.; da Costa, C. H. S.; Santana, A. R.; Dos Santos Carvalho, V.; do Nascimento, L. D.; Lima e Lima, A. H.; Neves Cruz, J.; Alves, C. N.; Lameira, J. Exploring the Potentiality of Natural Products from Essential Oils as Inhibitors of Odorant-Binding Proteins: A Structure- and Ligand-Based Virtual Screening Approach To Find Novel Mosquito Repellents. *ACS Omega* **2019**, *4* (27), 22475–22486. https://doi.org/10.1021/acsomega.9b03157.
9. Melo, N.; Capek, M.; Arenas, O. M.; Afify, A.; Yilmaz, A.; Potter, C. J.; Laminette, P. J.; Para, A.; Gallio, M.; Stensmyr, M. C. The Irritant Receptor TRPA1 Mediates the Mosquito Repellent Effect of Catnip. *Curr. Biol.* **2021**, *31* (9), 1988–1994.e5. https://doi.org/10.1016/j.cub.2021.02.010.
10. Reichert, W.; Ejercito, J.; Guda, T.; Dong, X.; Wu, Q.; Ray, A.; Simon, J. E. Repellency Assessment of *Nepeta cataria* Essential Oils and Isolated Nepetalactones on *Aedes aegypti*. *Sci. Rep.* **2019**, *9* (1), 1524. https://doi.org/10.1038/s41598-018-36814-1.
11. Birkett, M. A.; Hassanali, A.; Hoglund, S.; Pettersson, J.; Pickett, J. A. Repellent Activity of Catmint, *Nepeta cataria*, and Iridoid Nepetalactone Isomers against Afro-Tropical Mosquitoes, Ixodid Ticks and Red Poultry Mites. *Phytochemistry* **2011**, *72* (1), 109–114. https://doi.org/10.1016/j.phytochem.2010.09.016.
12. Sun, J. S.; Xiao, S.; Carlson, J. R. The Diverse Small Proteins Called Odorant-Binding Proteins. *Open Biol.* **2018**, *8* (12), 180208. https://doi.org/10.1098/rsob.180208.
13. Duarte, J. L.; Di Filippo, L. D.; Ribeiro, T. d. C.; Silva, A. C. d. J.; Hage-Melim, L. I. d. S.; Duchon, S.; Carrasco, D.; Pinto, M. C.; Corbel, V.; Chorilli, M. Effective Mosquito Repellents: Myrcene- and Cymene-Loaded Nanohydrogels against *Aedes aegypti*. *Pharmaceutics* **2024**, *16*, 1096. https://doi.org/10.3390/pharmaceutics16081096.
14. Pinnelli, G. R.; Terrado, M.; Hillier, N.; Lance, D.; Plettner, E. Synthesis of Isotopically Labelled Disparlure Enantiomers and Application to the Study of Enantiomer Discrimination in Gypsy Moth Pheromone-Binding Proteins. *Eur. J. Org. Chem.* **2019**, 2019, 10.1002/ejoc.201901164.
15. Nonkhwao, S.; Plettner, E.; Daduang, S. Protein-Ligand Binding and Structural Modelling Studies of Pheromone-Binding Protein-like Sol g 2.1 from *Solenopsis geminata* Fire Ant Venom. *Molecules* **2024**, *29* (5), 1033. https://doi.org/10.3390/molecules29051033.
16. Terrado, M.; Pinnelli, G. R.; Sanes, J.; Plettner, E. Binding Interactions, Structure–Activity Relationships and Blend Effects in Pheromone and Host Olfactory Detection of Herbivorous Lepidoptera. In *Insect Pheromone Biochemistry and Molecular Biology*; Springer, 2019; pp 1–25. https://doi.org/10.1007/978-3-030-05165-5_11.

 doi:10.20944/preprints202509.1531.v1

17. Sims, C.; Birkett, M. A.; Withall, D. M. Enantiomeric Discrimination in Insects: The Role of OBPs and ORs. *Insects* **2022**, *13*, 368. https://doi.org/10.3390/insects13040368.
18. Rao, P.; Goswami, D.; Rawal, R. M. Molecular Insights on Ar-Turmerone as a Structural, Functional and Pharmacophoric Analogue of Synthetic Mosquito Repellent DEET by Comprehensive Computational Assessment. *Sci. Rep.* **2022**, *12*, 15564. https://doi.org/10.1038/s41598-022-19901-2.
19. Moustakime, Y.; Hazzoumi, Z.; Amrani Joutei, K. Aromatization of Virgin Olive Oil by Seeds of *Pimpinella anisum* Using Three Different Methods: Physico-Chemical Change and Thermal Stability of Flavored Oils. *Grain Oil Sci. Technol.* **2021**, *4* (3), 108–124. https://doi.org/10.1016/j.gaost.2021.07.001.
20. Mohammadi, S.; Saharkhiz, M. Changes in Essential Oil Content and Composition of Catnip (*Nepeta cataria* L.) during Different Developmental Stages. *J. Essent. Oil Bear. Plants* **2013**, *14*, 396–400. https://doi.org/10.1080/0972060X.2011.10643592.
21. Gkinis, G.; Tzakou, O.; Iliopoulou, D.; Roussis, V. Chemical Composition and Biological Activity of *Nepeta parnassica* Oils and Isolated Nepetalactones. *Z. Naturforsch., C: J. Biosci.* **2003**, *58* (9–10), 681–686. https://doi.org/10.1515/znc-2003-9-1015.
22. Noosidum, A.; Chareonviriyaphap, T.; Chandrapatya, A. Synergistic Repellent and Irritant Effect of Combined Essential Oils on *Aedes aegypti* (L.) Mosquitoes. *J. Vector Ecol.* **2014**, *39* (2), 298–305. https://doi.org/10.1111/jvec.12104.
23. Manoharan, M.; Ng Fuk Chong, M.; Vaïtinadapoulé, A.; Frumence, E.; Sowdhamini, R.; Offmann, B. Comparative Genomics of Odorant Binding Proteins in *Anopheles gambiae*, *Aedes aegypti*, and *Culex quinquefasciatus*. *Genome Biol. Evol.* **2013**, *5* (1), 163–180. https://doi.org/10.1093/gbe/evs131.
24. Dassanayake, M. K.; Chong, C. H.; Khoo, T. J.; Figiel, A.; Szumny, A.; Choo, C. M. Synergistic Field Crop Pest Management Properties of Plant-Derived Essential Oils in Combination with Synthetic Pesticides and Bioactive Molecules: A Review. *Foods* **2021**, *10* (9), 2016. https://doi.org/10.3390/foods10092016.
25. Liu, Y.; Yang, X.; Gan, J.; Chen, S.; Xiao, Z. X.; Cao, Y. CB-Dock2: Improved Protein–Ligand Blind Docking by Integrating Cavity Detection, Docking and Homologous Template Fitting. *Nucleic Acids Res.* **2022**, *50* (W1), W159–W164. https://doi.org/10.1093/nar/gkac394.
26. Flores-Castañón, N.; Sarkar, S.; Banerjee, A. Structural, Functional, and Molecular Docking Analyses of Microbial Cutinase Enzymes against Polyurethane Monomers. *J. Hazard. Mater. Lett.* **2022**, *3*, 100063. https://doi.org/10.1016/j.hazl.2022.100063.
27. Ali, S.; et al. Identification and Evaluation of Inhibitors of Lipase from *Malassezia restricta* Using Virtual High-Throughput Screening and Molecular Dynamics Studies. *Int. J. Mol. Sci.* **2019**, *20* (4), 884. https://doi.org/10.3390/ijms20040884.
28. Nonkhwao, S.; Leaokittikul, D.; Patramanon, R.; et al. Revealing the pH-Dependent Conformational Changes in Sol g 2.1 Protein and Potential Ligands Binding. *Sci. Rep.* **2024**, *14*, 21179. https://doi.org/10.1038/s41598-024-72014-w.
29. Pires, D. E.; Blundell, T. L.; Ascher, D. B. pkCSM: Predicting Small-Molecule Pharmacokinetic and Toxicity Properties Using Graph-Based Signatures. *J. Med. Chem.* **2015**, *58* (9), 4066–4072. https://doi.org/10.1021/acs.jmedchem.5b00104.
30. Haleem, Z. M.; Yadav, S.; Cushion, M. L.; Tanner, R. J.; Carek, P. J.; Mainous, A. G. Exposure to N,N-Diethyl-Meta-Toluamide Insect Repellent and Human Health Markers: Population-Based Estimates from the National Health and Nutrition Examination Survey. *Am. J. Trop. Med. Hyg.* **2020**, *103* (2), 812–814. https://doi.org/10.4269/ajtmh.20-0226.
31. Lichman, B. R.; Godden, G. T.; Hamilton, J. P.; Palmer, L.; Kamileen, M. O.; Zhao, D.; Vaillancourt, B.; Wood, J. C.; Sun, M.; Kinser, T. J.; Henry, L. K.; Rodriguez-Lopez, C.; Dudareva, N.; Soltis, D. E.; Soltis, P. S.; Buell, C. R.; O'Connor, S. E. The Evolutionary Origins of the Cat Attractant Nepetalactone in Catnip. *Sci. Adv.* **2020**, *6* (20), eaba0721. https://doi.org/10.1126/sciadv.aba0721.
32. Bernier, U. R.; Furman, K. D.; Kline, D. L.; Allan, S. A.; Barnard, D. R. Comparison of Contact and Spatial Repellency of Catnip Oil and N,N-Diethyl-3-Methylbenzamide (DEET) against Mosquitoes. *J. Med. Entomol.* **2005**, *42* (3), 306–311. https://doi.org/10.1603/0022-2585(2005)042[0306:cocasr]2.0.co;2.

 doi:10.20944/preprints202509.1531.v1

33. Chauhan, K. R.; Klun, J. A.; Debboun, M.; Kramer, M. Feeding Deterrent Effects of Catnip Oil Components Compared with Two Synthetic Amides against *Aedes aegypti*. *J. Med. Entomol.* **2005**, *42* (4), 643–646. https://doi.org/10.1603/0022-2585(2005)042[0643:fdeoco]2.0.co;2.
34. Leal, W. S. Odorant Reception in Insects: Roles of Receptors, Binding Proteins, and Degrading Enzymes. *Annu. Rev. Entomol.* **2013**, *58*, 373–391. https://doi.org/10.1146/annurev-ento-120811-153635.
35. Batume, C.; Mulongo, I. M.; Ludlow, R.; Ssebaale, J.; Randerson, P.; Pickett, J. A.; Mukisa, I. M.; Scofield, S. Evaluating Repellence Properties of Catnip Essential Oil against the Mosquito Species *Aedes aegypti* Using a Y-Tube Olfactometer. *Sci. Rep.* **2024**, *14*, 2269. https://doi.org/10.1038/s41598-024-52715-y.
36. Barnard, D. R.; Xue, R. D. Laboratory Evaluation of Mosquito Repellents against *Aedes albopictus*, *Culex nigripalpus*, and *Ochlerotatus triseriatus* (Diptera: Culicidae). *J. Med. Entomol.* **2004**, *41* (4), 726–730. https://doi.org/10.1603/0022-2585-41.4.726.
37. Souto, A. L.; Sylvestre, M.; Tölke, E. D.; Tavares, J. F.; Barbosa-Filho, J. M.; Cebrián-Torrejón, G. Plant-Derived Pesticides as an Alternative to Pest Management and Sustainable Agricultural Production: Prospects, Applications and Challenges. *Molecules* **2021**, *26*, 4835. https://doi.org/10.3390/molecules26164835.
38. Angerosa, F.; d'Alessandro, N.; Konstantinou, P.; Di Giacinto, L. GC-MS Evaluation of Phenolic Compounds in Virgin Olive Oil. *J. Agric. Food Chem.* **1995**, *43* (7), 1802–1807. https://doi.org/10.1021/jf00055a010.
39. Logan, J. G.; Stanczyk, N. M.; Hassanali, A.; Kemei, J.; Santana, A. E.; Ribeiro, K. A.; Pickett, J. A.; Mordue Luntz, A. J. Arm-in-Cage Testing of Natural Human-Derived Mosquito Repellents. *Malar. J.* **2010**, *9*, 239. https://doi.org/10.1186/1475-2875-9-239.
40. Isman, M. B. Botanical Insecticides: For Richer, for Poorer. *Pest Manag. Sci.* **2008**, *64* (1), 8–11. https://doi.org/10.1002/ps.1470
41. Chen, X.; Shang, S.; Yan, F.; Jiang, H.; Zhao, G.; Tian, S.; Chen, R.; Chen, D.; Dang, Y. Antioxidant Activities of Essential Oils and Their Major Components in Scavenging Free Radicals, Inhibiting Lipid Oxidation and Reducing Cellular Oxidative Stress. *Molecules* **2023**, *28* (11), 4559. https://doi.org/10.3390/molecules28114559.
42. Tsitsanou, K. E.; Thireou, T.; Drakou, C. E.; Koussis, K.; Keramioti, M. V.; Leonidas, D. D.; Eliopoulos, E.; Iatrou, K.; Zographos, S. E. *Anopheles gambiae* Odorant Binding Protein Crystal Complex with the Synthetic Repellent DEET: Implications for Structure-Based Design of Novel Mosquito Repellents. *Cell. Mol. Life Sci.* **2012**, *69* (2), 283–297. https://doi.org/10.1007/s00018-011-0745-z.
43. Jia, Z.; Qin, Z.; Ge, X.; Xu, Y.; Chen, Z. The Odorant-Binding Proteins AspiOBP1 and AspiOBP2 in *Aleurocanthus spiniferus* Are Involved in the Perception of Host Volatiles. *Int. J. Mol. Sci.* **2025**, *26* (18), 8784. https://doi.org/10.3390/ijms26188784.
44. Kröber, T.; Koussis, K.; Bourquin, M.; Tsitoura, P.; Konstantopoulou, M.; Awolola, T. S.; Dani, F. R.; Qiao, H.; Pelosi, P.; Iatrou, K.; Guerin, P. M. Odorant-Binding Protein-Based Identification of Natural Spatial Repellents for the African Malaria Mosquito *Anopheles gambiae*. *Insect Biochem. Mol. Biol.* **2018**, *96*, 36–50. https://doi.org/10.1016/j.ibmb.2018.03.008.
45. Ghavami, M. B.; Khoeini, S.; Djadid, N. D. Molecular Characteristics of Odorant-Binding Protein 1 in *Anopheles maculipennis*. *Malar. J.* **2020**, *19* (1), 29. https://doi.org/10.1186/s12936-019-3058-6.
46. Cong, Y.; Li, M.; Feng, G.; et al. Trypsin-Ligand Binding Affinities Calculated Using an Effective Interaction Entropy Method under Polarized Force Field. *Sci. Rep.* **2017**, *7*, 17708. https://doi.org/10.1038/s41598-017-17868-z.
47. Kots, E.; Shore, D. M.; Weinstein, H. Simulation of pH-Dependent Conformational Transitions in Membrane Proteins: The CLC-ec1 Cl^-/H^+ Antiporter. *Molecules* **2021**, *26* (22), 6956. https://doi.org/10.3390/molecules26226956.
48. Leal, W. S.; Chen, A. M.; Erickson, M. L. Selective and pH-Dependent Binding of a Moth Pheromone to a Pheromone-Binding Protein. *J. Chem. Ecol.* **2005**, *31* (10), 2493–2499. https://doi.org/10.1007/s10886-005-7458-4.

 doi:10.20944/preprints202509.1531.v1

49. Sen, D.; Debnath, B.; Debnath, P.; et al. Identification of Potential Edible Mushroom as SARS-CoV-2 Main Protease Inhibitor Using Rational Drug Designing Approach. *Sci. Rep.* **2022**, *12*, 1503. https://doi.org/10.1038/s41598-022-05349-x.
50. Sudakin, D. L.; Trevathan, W. R. DEET: A Review and Update of Safety and Risk in the General Population. *J. Toxicol. Clin. Toxicol.* **2003**, *41* (6), 831–839. https://doi.org/10.1081/clt-120025348.
51. Osimitz, T. G.; Murphy, J. V. Neurological Effects Associated with Use of the Insect Repellent N,N-Diethyl-m-toluamide (DEET). *J. Toxicol. Clin. Toxicol.* **1997**, *35* (5), 435–441. https://doi.org/10.3109/15563659709001224.
52. Khajeh, M.; Yamini, Y.; Shariati, S. Comparison of Essential Oils Compositions of *Nepeta persica* Obtained by Supercritical Carbon Dioxide Extraction and Steam Distillation Methods. *Food Bioprod. Process.* **2010**, *88* (2–3), 227–232. https://doi.org/10.1016/j.fbp.2008.11.003.
53. Borlace, G.; Singh, R.; Seubsasana, S.; Chantaranotahi, P.; Thongkham, E.; Aiemsaard, J. Antimicrobial Effects of Catnip (*Nepeta cataria* L.) Essential Oil against Canine Skin Infection Pathogens. *Vet. World* **2024**, *17*, 585–592. https://doi.org/10.14202/vetworld.2024.585-592.
54. Mao, Y.; Xu, X.; Xu, W.; Ishida, Y.; Leal, W. S.; Ames, J. B.; Clardy, J. Crystal and Solution Structures of an Odorant-Binding Protein from the Southern House Mosquito Complexed with an Oviposition Pheromone. *Proc. Natl. Acad. Sci. U.S.A.* **2010**, *107* (44), 19102–19107. https://doi.org/10.1073/pnas.1012274107.
55. Leite, N. R.; Krogh, R.; Xu, W.; Ishida, Y.; Iulek, J.; Leal, W. S.; Oliva, G. Structure of an Odorant-Binding Protein from the Mosquito *Aedes aegypti* Suggests a Binding Pocket Covered by a pH-Sensitive "Lid". *PLoS One* **2009**, *4* (11), e8006. https://doi.org/10.1371/journal.pone.0008006.
56. Yekeen, A. A.; Durojaye, O. A.; Idris, M. O.; Muritala, H. F.; Arise, R. O. CHAPERONg: A Tool for Automated GROMACS-Based Molecular Dynamics Simulations and Trajectory Analyses. *Comput. Struct. Biotechnol. J.* **2023**, *21*, 4849–4858. https://doi.org/10.1016/j.csbj.2023.09.024.
57. Tyagi, R.; Paul, A.; Raj, V. S.; Ojha, K. K.; Kumar, S.; Panda, A. K.; Chaurasia, A.; Yadav, M. K. A Drug Repurposing Approach to Identify Therapeutics by Screening Pathogen Box Exploiting SARS-CoV-2 Main Protease. *Chem. Biodivers.* **2023**, *20* (2), e202200600. https://doi.org/10.1002/cbdv.202200600.